Mechanical and Mode-I Fracture Properties of Epoxy-Clay Nanocomposites Prepared by Ultrasonic Dispersion Method

Mohammad T. Bashar and Pierre Mertiny
University of Alberta, Mechanical Engineering Department, Edmonton, Canada
Email: {bashar, pmertiny}@ualberta.ca

***Abstract*—In the present study, the effect of organically modified nanoclay on mechanical and mode-I fracture behavior of epoxy-clay nanocomposite was investigated. In epoxy few exfoliated and mostly intercalated nanoclay structures were observed when I.30E clay was dispersed by an ultrasonic blending method. The epoxy-clay nanocomposites exhibited superior tensile stiffness with slight reduction in tensile strength. However, the exfoliated and intercalated nanoclay did not influence the fracture energy of the epoxy-clay nanocomposite, as crack deflection was found to be the predominant crack resistance mechanism that resulted insignificant energy dissipation. It was also manifested that the presence of nanoclay in the matrix has less pronounced effect on delamination fracture toughness, although decreasing fiber volume fraction improved interlaminar fracture energy by aiding unconstrained matrix deformation.**

***Index Terms*—clay, epoxy, nanocomposite, microstructure, mechanical property, fracture behavior**

I. Introduction

Polymer-clay nanocomposites are inorganic/organic hybrids. Nanoscale dispersion of the layered silicate into a polymer resin, thus generating polymer-clay nanocomposite results in exceptional enhancements in material properties relative to the micro and fiber composites [1]-[6]. Normally, polymer-clay nanocomposites contain very small amount of the nano-dispersants, about 2-3vol%, consequently the finished products are light-weight (owing to their comparable property enhancement) compared to traditionally filled composites. Silicate clay (e.g. montmorillonite, hectorite and saponite) used for nanocomposite preparation falls into the general class of phyllosilicates that has a 2:1 layered type structure consisting of either hydrous magnesium or aluminum silicates [3].

Based on the combination of different constituents chosen (e.g. layered silicate, organic cation and polymer) and processing condition adopted organoclay can be transformed to give rise micro or nanostructured morphologies inside a polymer matrix. A mixture of polymer and inorganic silicate does not necessarily produce a nanocomposite, rather the immiscibility or partial miscibility between constituents in most cases develop conventional microcomposites (i.e. phase-separated structure) having clay microaggregates evenly or unevenly distributed in the matrix. In a compatible polymer and clay system, if the monomers or oligomers are able to migrate into the clay galleries that can leads to two more fundamental clay morphologies, i.e. intercalated and exfoliated nanocomposites. Exfoliated clay configuration brings about the highest degree of property enhancement that is possible in the polymer-clay nanocomposites. For successful processing of epoxy-clay nanocomposites, it is a prerequisite that enough epoxy monomers or oligomers must be pre-intercalated into the clay galleries in order to participate in the intragallery polymerization that must also be comparable or higher than the extragallery polymerization rate. The extent of clay layer separation depends on chain length of the organic cations, acidity of the organic cation and clay layer charge density [7]. The choice of epoxy resin and curing agent plays an important role in influencing exfoliation of the silicate layer. Furthermore, the degree of exfoliation and intercalation is dependent on mixing and curing conditions, such as mixing time, curing time and temperature [7]. Synthesis approach for preparation of epoxy-clay nanocomposites involves several established fabrication methodologies: exfoliation-adsorption, in-situ intercalative polymerization and melt intercalation [3], [8].

Polymer-clay nanocomposites have significantly improved physical and mechanical properties, which can be advantageous for specific engineering applications and in specialty products. The versatility in nanocomposite properties comes in many different forms and parameters, such as mechanical properties (stiffness, strength, fracture and impact resistance), dimensional stability, barrier properties (for gas and liquid), flame retardance, chemical resistance, optical properties and thermal stability [9]. On study of mechanical properties of clay-reinforced nanocomposite, Lan and Pinnavaia [5] documented almost 10 fold increase in modulus and strength of a rubbery epoxy for a 15wt% addition of organoclay. In an exfoliated nanocomposite the impressive increase in stiffness is attributed to a mechanism of shear deformation and stress transfer to the high stiffness and high aspect ratio individual silicate platelets [5], [7].

Manuscript received November 11, 2013; revised February 15, 2014.

doi: 10.12720/ijmse.2.2.87-92

Kornmann *et al.* [10] reported simultaneous improvements in fracture toughness and Young's modulus of epoxy-clay nanocomposites, while maintaining the tensile strength constant. Fracture toughness of epoxy-clay nanocomposites has shown mixed results; uniformly dispersed phase-separated or intercalated nanoclay is generally known to enhance toughness as observed by Kornmann *et al.* [11] and Zerda and Lesser [12], while insignificant toughness improvements are reported for perfectly exfoliated layered silicate [13]. In nanoclay modified epoxy, crack deflection and bifurcation [14]-[16], crack pinning [14]-[15] and matrix deformation [14]-[16] are the most commonly observed crack resistance mechanisms.

In this paper, the effect of nanoclay on the microstructure, mechanical and fracture behavior of epoxy-clay nanocomposite was studied. This research involved synthesis, characterization and property evaluation of epoxy-clay nanocomposites and basalt fiber-reinforced epoxy nanocomposite laminates modified with I.30E organophilic nanoclay.

II. Experimental Procedure

A. Material and Preparation of the Epoxy-Clay Nanocomposite

Epoxy resin EPON 826 and curing agent EPIKURE 9551 were received from Momentive (Columbus, Ohio, USA). Primary alkylammonium ion modified organoclay Nanomer I.30E ($CH_3(CH_2)_{17}NH_3$-MMT) was supplied by Nanocor Inc. (Hoffman Estates, Illinois, USA).

At first, the I.30E nanoclay was dried in an oven at 120 ℃ for a period of 24 hours, and subsequently allowed to cool down to room temperature. Then a specified amount of dried nanoclay was added to acetone. The mixture was then held at the room temperature for six hours. During this time, diffusion of solvent into the clay interlayers and swelling occurred. The solution was then mixed with the desired amount of preheated EPON 826 resin at 60 ℃, and subsequently sonicated at 80 ℃ for eight hours with a Branson model S-75 Sonifier (Branson Ultrasonics Corporation, Danbury, CT, USA) [17]-[18]. Afterward, the solution was mechanically blended for two hours. Acetone was removed from the solution by vacuum extraction performed at 80kPa for 10~20 minutes. Finally, the epoxy-clay blend was mixed with EPIKURE 9551 curing agent, which was followed by mechanical mixing at 60 ℃ for five minutes. Any entrapped air and volatiles formed during mixing with the curing agent were evacuated by a vacuum pump operated at 80kPa for 10~20 minutes. The final mixture was then poured into a steel mold for curing. The solidification of the epoxy and nanoclay blend occurred in an oven at 120 ℃ for two hours. Nanocomposites containing 1wt%, 2wt%, and 3wt% I.30E clay were produced according to this procedure. Fig. 1 shows a process flow diagram of the epoxy-clay nanocomposite preparation steps.

Basalt fiber-reinforced epoxy nanocomposite laminates were fabricated by filament winding method. A numerically controlled filament winder was used to wound continuous fiber strands onto a rotating flat mandrel having a dimension of 15cm by 20cm. Laminates were made of 8 plies, each about ~0.625mm thick with unidirectional lay-up having a fiber configuration of $[\pm 89.5_4]_T$. A 50 μm thin ethylene tetrafluoroethylene film insert was placed at the mid-plane of the laminates as a crack initiator. Finally, the composite was cured in an oven at 120 ℃ for two hours aided by vacuum bagging technique to soak out the excess resin. Laminates made of neat and 1 and 3wt% I.30E modified epoxy were processed by following the same procedure as mentioned above. 120mm long and 20mm wide test specimens were cut from the laminates, which also includes a delamination insert length of 50mm. The fiber volume fraction varied within the range of 0.5 to 0.64, which was measured by resin burn-out test.

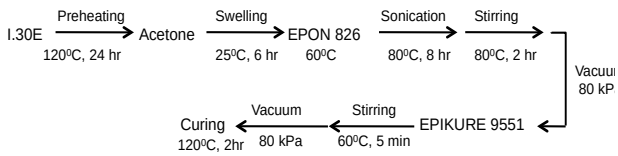

Figure 1. Process flow diagram of nanocomposite fabrication method

B. Characterization and Experimental Methods

Wide angle X-ray diffraction (WAXD) study of the nanocomposites was performed by Rigaku Geigerflex 2173 (Rigaku Corporation, Tokyo, Japan) diffractometer. The diffractometer is fitted with a Co-tube as an X-ray source and a graphite monochromator to filter K-beta wavelength. Tests were run at 40kV and 30mA, and the samples were scanned between 2θ = 1 to 30 °by changing the angle of incidence at a rate of 0.008 2θsec^{-1}.

Morphology of the cured epoxy nanocomposite samples was examined in a Morgagni 268 (FEI, Hillsboro, Oregon, USA) transmission electron microscope (TEM) with an acceleration voltage of 80kV. Ultrathin 40~60nm sections were cut by a diamond knife of the Reichert-Jung Ultracut E microtome (C. Reichert Optische Werke AG, Vienna, Austria). These ultrathin sections were then laid onto 300 mesh copper grids and placed inside the TEM for scanning.

Fracture surface of the nanocomposites was examined by a JEOL 6301F (JEOL Ltd., Tokyo, Japan) field emission scanning electron microscope (SEM) at an acceleration voltage of 5kV. Before scanning a conductive coating of gold was applied on the fracture surfaces of single edge notch bend (SENB) specimens.

Tensile modulus and strength of the nanocomposites were determined according to the standard ASTM D 638-03 using a MTS 810 machine (MTS Systems Corporation, Eden Prairie, MN, USA). Dog-bone shaped specimen was tested under load control condition at a constant loading rate of 4.5N/sec.

Mode-I fracture toughness of SENB specimens was determined according to the procedure described in the standard ASTM D 5045-99. The critical stress intensity factor, K_{IC} and strain energy release rate, G_{IC} were determined according to linear elastic fracture mechanics principle. Equation (1) was used to calculate fracture

toughness. Specimens were loaded under plane-strain condition in three-point bending until failure occurred from an initially prepared sharp pre-crack. Testing was conducted using a MTS 810 universal tester at a crosshead speed of 0.2mm/min.

$$K_I = \left(\frac{P}{BW^{1/2}}\right) f(x) \quad with, x = \frac{a}{W} \tag{1}$$

$$f(x) = 6x^{1/2} \frac{[1.99 - x(1-x)(2.15 - 3.93x + 2.7x^2)]}{(1+2x)(1-x)^{3/2}}$$

where $f(x)$ is the geometric factor, P is the failure load, B is the specimen thickness, W is the specimen width and a is the overall crack length. The strain energy release rate, G_{IC} was determined from equation (2).

$$G_Q = \frac{U}{BW\phi} \tag{2}$$

where U is the energy estimated by integrating the area under the load versus load-point displacement curve, and the energy calibration factor can be expressed as ϕ.

Mode-I interlaminar fracture toughness, G_{IC} of double-cantilever beam (DCB) specimens was estimated according to the ASTM D 5528-01 standard. All tests were performed under displacement control condition on a MTS 810 universal tester. The samples were delaminated to a length of 70mm from the insert edge at a loading speed of 2.5mm/min, and subsequently unloaded at 5mm/min. Energy required for delamination initiation as well steady-state crack propagation was calculated. Strain energy release rate was determined according to the modified beam theory by using the following formula.

$$G_{IC} = \frac{3P_1\delta}{2b(a_1 + |\Delta|)} \tag{3}$$

where P_1 is the load, δ is the load point displacement, b is the specimen width, a_1 is the delamination length and Δ is the delamination correction factor.

III. Results and Discussion

A. Microstructure of the Epoxy-Clay Nanocomposite

In this study, WAXD and TEM methods were employed to investigate microstructure of the epoxy-clay nanocomposites. From the X-ray diffraction (XRD) pattern of the primary alkylammonium ion treated nanoclay I.30E, the *d*-spacing, d_{001} was estimated as 2.23nm representing the prominent diffraction peak in Fig. 2. In the same figure, XRD traces of the cured nanocomposites containing various weight fractions of the I.30E clay are presented. It was observed that the presence of 1wt% and 2wt% I.30E clay in the nanocomposites did not produce any distinct diffraction peak, whereas a prominent peak indicating an interlayer spacing of d_{001}=2.73nm was found for the nanocomposite made with 3wt% clay. Considering the detection limit of WAXD ($2\theta \geq 1$), it is understood that the absence of a reflection peak suggests either an exfoliated or an intercalated nanocomposite structure having an interlayer distance greater than 8.83nm.

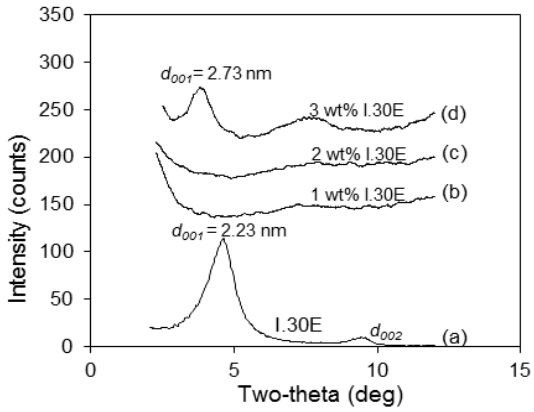

Figure 2. X-ray diffraction patterns of the (a) I.30E clay and epoxy-clay nanocomposites: (b), (c) and (d).

The TEM image in Fig. 3(a) shows that the ultrasonic dispersion produced partially exfoliated and mainly intercalated structures in the nanocomposite containing 1wt% I.30E clay. The same picture displays exfoliated disordered individual 1nm thick silicate platelets as well as laminated parallel platelets with a layer separation of 10~15nm. In a study, Lan *et al.* [19] deduced that clay interlayer separation is affected by the catalytic influence of the acidic alkylammonium ion during epoxy-amine curing reaction. Therefore, it can be inferred that during processing of epoxy-clay nanocomposite, intragallery catalytic polymerization rate was comparatively higher than the extragallery polymerization that resulted increase in I.30E clay interlayer distance [20]. The low magnification TEM image in Fig. 3(b) shows submicron size intercalated clay tactoids uniformly dispersed in the epoxy matrix.

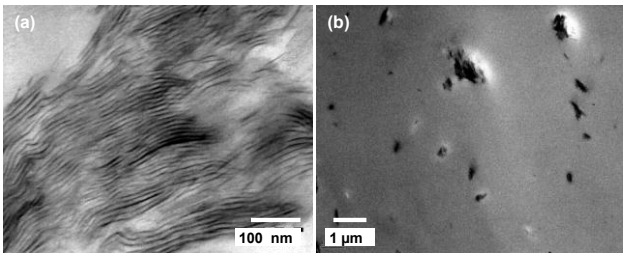

Figure 3. TEM micrographs of the epoxy-clay nanocomposites containing (a) 1wt% and (b) 2wt% I.30E clay

B. Tensile Properties of the Epoxy-Clay Nanocomposite

All nanocomposite samples having varying compositions of the I.30E clay were subjected to uniaxial tensile testing. The influence of the nanoclay weight percentages on mechanical properties of the cured nanocomposites is shown in Fig. 4. At least four specimens were tested for each nanocomposite sample, and in the graph the error bars represent one standard deviation. Tensile modulus and strength of the unfilled epoxy were determined as 2.8GPa and 82MPa respectively. It was observed that stiffness increased significantly with increasing I.30E content. An approximately 20% increase in modulus for the nanocomposites was the observed maximum for a modifier loading of 3wt%. It was ascertained that the

presence of uniformly dispersed exfoliated rigid nanoplatelets and well-intercalated smaller submicron size clay particles resulted in substantial stiffness improvement [21]. As expected strength values remained almost unchanged with slight reduction at higher clay loadings as shown in Fig. 4.

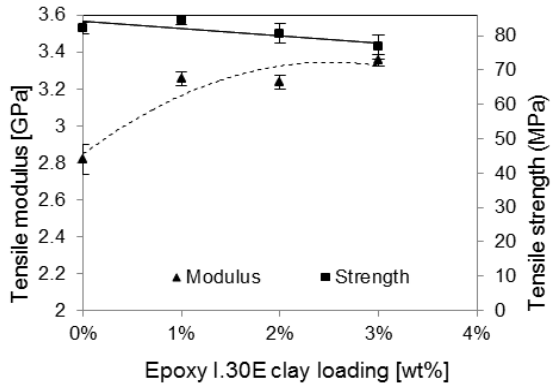

Figure 4. Tensile modulus and strength of the epoxy-clay nanocomposites as a function of I.30E clay content

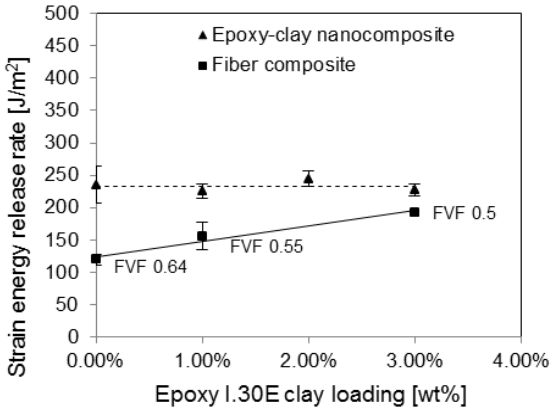

Figure 5. Variations in fracture energy of the epoxy-clay nanocomposites and fiber composites with I.30E clay loading

C. Fracture Properties of the Epoxy-Clay Nanocomposite

Fig. 5 illustrates fracture energy of the neat epoxy and I.30E clay filled epoxy as a function of clay content. The fracture toughness and strain energy of the neat epoxy were measured as 0.78MPa·m$^{0.5}$ and 240J/m^2 respectively. It was observed that critical strain energy release rate measured for the nanocomposite samples remained almost unchanged with increasing I.30E content. In a study, Zilg *et al.* [22] had inferred that in a nanocomposite the degree of nanoclay exfoliation is directly related to its stiffness increase, while fracture toughness is inversely affected by the exfoliation state. Therefore, the intercalated and/or phase-separated microparticles would be more effective in impeding crack propagation than the exfoliated clay platelets [11], [13]. Previous studies conducted on fracture behavior of epoxy-clay nanocomposite have found evidence of occurrence of such crack resistance mechanisms as crack pinning, crack deflection and matrix deformation [14]-[16].

Fracture surface micrographs (i.e. SEM) of the pure epoxy and nanoclay modified epoxy are displayed in Fig. 6. The neat epoxy fracture surface shown is clearly plain and featureless, which is typical of a brittle fracture in an amorphous material. Compared to the neat resin, fracture surface of I.30E modified epoxy is extensively uneven, rough and coarse, which are definite signs of crack resistance through a distorted and perturbed path. The fracture surface showing perturbed and tortuous crack path indicates the occurrence of crack deflection mechanism when path of a propagating crack is obstructed by both the intercalated parallel platelets and exfoliated isolated platelets. In this study we expected an increase in fracture toughness as documented by Zerda and Lesser [12] who showed that intercalated nanoclay resulted in crack deflection through diverting crack in a tortuous path with the creation of new surface area. But, the intercalated clay structures observed in this study are mostly composed of smaller submicron size intercalated clay tactoids that behaved analogous to exfoliated platelets. This behavior is also evidenced through significant improvements in the nanocomposite stiffness values [17]. In Fig. 6 (c) and Fig. 6(d), the fracture surfaces become comparatively rough as the clay loading increases. But, river markings running from the deflected crack paths are actually very shallow, and fracture energy values remained unchanged. Therefore, we inferred that the insignificant improvement in fracture energy is mainly due to the crack deflection that was found to be the only operative crack resistance mechanism in this particular epoxy system, this has been observed in the past by others for epoxy [23].

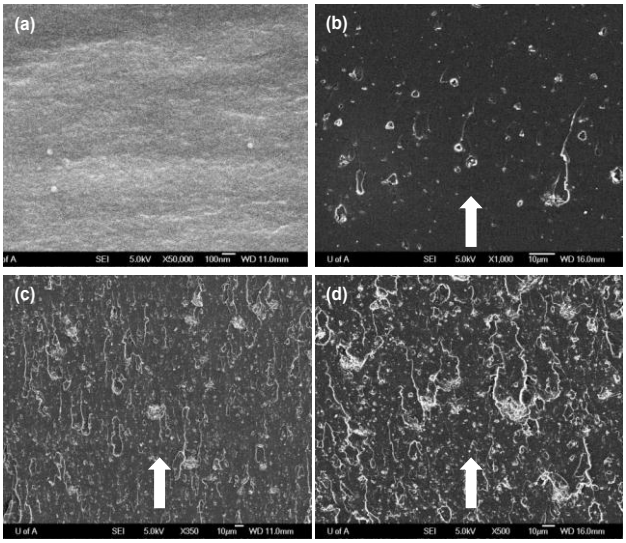

Figure 6. SEM micrographs of the (a) neat epoxy and nanocomposites containing (b) 1wt%, (c) 2wt% and (d) 3wt% I.30E clay.

D. Interlaminar Fracture Toughness of the Fiber Composite

Interlaminar crack initiation energy of the fiber composites is presented in Fig. 5, with respective I.30E nanoclay content and fiber volume fraction (FVF). It was observed that in the fiber composite nanoclay dispersion enhanced interlaminar crack initiation energy, but the

values are lower than the bulk nanocomposite fracture energy values. This improvement is mostly due to the increase in fiber volume fractions in these laminates, because for the nanoclay filled bulk nanocomposites it was observed that fracture energy values remained unchanged. Lee [24] studied interlaminar fracture behaviour of glass and graphite fiber epoxy laminates, and observed an increase in delamination initiation energy with increasing resin content (from 0.27 to 0.40). In a study of interlaminar fracture in fiber composites, Hunston [25] hypothesized that the rigid fibers restrict the development of a plastic zone at the crack-tip. Hence, findings from this study lead to the inference that the improvement in laminate delamination fracture energy with increasing resin content suggests existence of such a constraining influence by the fibers. As the fiber volume fraction decreases in a composite laminate the resin rich region between adjacent fibers gets bigger, this reduces the constraining effect of the fibers.

IV. Conclusion

In this study, the microstructure and mechanical properties of epoxy-clay nanocomposites and fiber composites modified with organophilic layered silicate clay were explored. In cured epoxy a predominantly intercalated and partially exfoliated structure was observed for I.30E nanoclay. Tensile and fracture testing indicated that the nanoclay filled epoxy-clay nanocomposites exhibited superior tensile stiffness, while strain energy release rate remained unchanged. A combined reinforcing effect of the exfoliated clay nano-layers and intercalated submicron clay tactoids is thought responsible for enhancement in modulus, while fracture energy was found to be independent of clay layer separation. Mode-I interlaminar fracture toughness test indicated that increasing nanoclay concentration did not improve crack initiation resistance, but decreasing fiber volume fraction enhanced interlaminar fracture energy. The differences in fracture resistance behaviour between the bulk composite and fiber composite are due to the fibers restricting the stress field ahead of the crack-tip.

References

[1] Y. Kojima, A. Usuki, M. Kawasumi, *et al.*, "Mechanical properties of nylon 6-clay hybrid," *Journal of Materials Research*, vol. 8, no. 5, pp. 1185-1189, May 1993.

[2] A. Okada and A. Usuki, "The chemistry of polymer-clay hybrids," *Materials Science & Engineering: C*, vol. 3, no. 2, pp. 109-115, Nov. 1995.

[3] F. Hussain, M. Hojjati, M. Okamoto, and R. E. Gorga, "Review article: Polymer-matrix nanocomposites, processing, manufacturing, and application: An overview," *Journal of Composite Materials*, vol. 40, no. 17, pp. 1511-1575, Sep. 2006.

[4] E. P. Giannelis, "Polymer layered silicate nanocomposites," *Advanced Materials*, vol. 8, no. 1, pp. 29-35, Jan. 1996.

[5] T. Lan and T. J. Pinnavaia, "Clay-reinforced epoxy nanocomposites," *Chemistry of Materials*, vol. 6, no. 12, pp. 2216-2219, Dec. 1994.

[6] P. B. Messersmith and E. P. Giannelis, "Synthesis and characterization of layered silicate-epoxy nanocomposites," *Chemistry of Materials*, vol. 6, no. 10, pp. 1719-1725, Oct. 1994.

[7] T. J. Pinnavaia, T. Lan, Z. Wang, H. Shi, and P. D. Kaviratna, "Clay-reinforced epoxy nanocomposites: synthesis, properties, and mechanism of formation," in *Nanotechnology: ACS Symposium Series*, vol. 622, G. M. Chow and K. E. Gonsalves, Ed. Washington, DC: American Chemical Society, 1996, pp. 250-261.

[8] M. Alexandre and P. Dubois, "Polymer-layered silicate nanocomposites: Preparation, properties and uses of a new class of materials," *Materials Science and Engineering R-Reports*, vol. 28, no. 1, pp. 1-63, Jun. 2000.

[9] O. Becker and G. P. Simon, "Epoxy layered silicate nanocomposites," *Advances in Polymer Science*, vol. 179, pp. 29-82, 2005.

[10] X. Kornmann, R. Thomann, R. Mülhaupt, J. Finter, and L. A. Berglund, "High performance epoxy-layered silicate nanocomposites," *Polymer Engineering and Science*, vol. 42, no. 9, pp. 1815-1826, Sep. 2002.

[11] X. Kornmann, R. Thomann, R. Mülhaupt, J. Finter, and L. Berglund, "Synthesis of amine-cured, epoxy-layered silicate nanocomposites: the influence of the silicate surface modification on the properties," *Journal of Applied Polymer Science*, vol. 86, no. 10, pp. 2643-2652, Dec. 2002.

[12] A. S. Zerda and A. J. Lesser, "Intercalated clay nanocomposites: morphology, mechanics, and fracture behavior," *Journal of Polymer Science Part B: Polymer Physics*, vol. 39, no. 11, pp. 1137-1146, Jun. 2001.

[13] H. Miyagawa and L. T. Drzal, "The effect of chemical modification on the fracture toughness of montmorillonite clay/epoxy nanocomposites," *Journal of Adhesion Science and Technology*, vol. 18, no. 13, pp. 1571-1588, 2004.

[14] N. A. Siddiqui, R. S. C. Woo, J.-K. Kim, C. C. K. Leung, and A. Munir, "Mode I interlaminar fracture behaviour and mechanical properties of CFRPs with nanoclay-filled epoxy matrix," *Composites Part A: Applied Science and Manufacturing*, vol. 38, no. 2, pp. 449-460, 2007.

[15] W. Liu, S. V. Hoa, and M. Pugh, "Organoclay-modified high performance epoxy nanocomposites," *Composite Science and Technology*, vol. 65, no. 2, pp. 307-316, Feb. 2005.

[16] T. Liu, W. C. Tjiu, Y. Tong, *et al.*, "Morphology and fracture behaviour of intercalated epoxy/clay nanocomposites," *Journal of Applied Polymer Science*, vol. 94, no. 3, pp. 1236-1244, Nov. 2004.

[17] M. T. Bashar, U. Sundararaj, and P. Mertiny, "Study of matrix micro-cracking in nanoclay and acrylic tri-block-copolymer modified epoxy/basalt fiber-reinforced pressure-retaining structures," *Express polymer letters*, vol. 5, no. 10, pp. 882-896, 2011.

[18] M. T. Bashar, U. Sundararaj, and P. Mertiny, "Microstructure and mechanical properties of epoxy hybrid nanocomposites modified with acrylic tri-block-copolymer and layered-silicate nanoclay," *Composites Part A: Applied Science and Manufacturing*, vol. 43, no. 6, pp. 945-954, Jun. 2012.

[19] T. Lan, P. D. Kaviratna, and T. J. Pinnavaia, "Mechanism of clay tactoid exfoliation in epoxy-clay nanocomposites," *Chemistry of Materials*, vol. 7, no. 11, pp. 2144-2150, Nov. 1995.

[20] J. M. Brown, D. Curliss, and R. A. Vaia, "Thermoset-layered silicate nanocomposites. Quaternary ammonium montmorillonite with primary diamine cured epoxies," *Chemistry of Materials*, vol. 12, no. 11, pp. 3376-3384, Nov. 2000.

[21] A. Yasmin, J. L. Abot, and I. M. Daniel, "Processing of clay/epoxy nanocomposites by shear mixing," *Scripta Materialia*, vol. 49, no. 1, pp. 81-86, Jul. 2003.

[22] C. Zilg, R. Mülhaupt, and J. Finter, "Morphology and toughness/stiffness balance of nanocomposites based upon anhydride-cured epoxy resins and layered silicates," *Macromolecular Chemistry and Physics*, vol. 200, no. 3, pp. 661-670, Mar. 1999.

[23] A. C. Garg and Y. W. Mai, "Failure mechanisms in toughened epoxy resins-A review," *Composites Science and Technology*, vol. 31, no. 3, pp. 179-223, 1988.

[24] S. LEE, "A comparison of fracture-toughness of matrix controlled failure modes - delamination and transverse cracking," *Journal of Composite Materials*, vol. 20, no. 2, pp. 185-196, Mar. 1986.

[25] D. L. Hunston, "Composite interlaminar fracture: Effect of matrix fracture energy," *Composites Technology Review*, vol. 6, no. 4, pp. 176-180, 1984.

Mohammad T. Bashar obtained his PhD degree in Mechanical Engineering from University of Alberta, Canada in the year of 2013. He obtained an MSc degree in Chemical Engineering from University of New Brunswick, Canada in the year of 2005. He graduated with a BSc degree in Chemical Engineering from Bangladesh University of Engineering and Technology, Bangladesh in the year of 2002.
Currently, he is working as a POSTDOCTORAL FELLOW at the University of Alberta. His research interests include polymer nanocomposites and fiber-reinforced polymer composite structures with a special focus on enhancing mechanical properties and performance under demanding operating conditions.

Pierre Mertiny obtained his PhD degree in Mechanical Engineering from University of Alberta, Canada in the year of 2005. He obtained a Dipl.-Ing. degree in Mechanical Engineering from University of Hannover, Germany in the year of 1999.
Presently, he is working as an ASSOCIATE PROFESSOR in mechanical engineering at University of Alberta. His research interests focus on advanced polymer composites, including material behavior, damage prediction, and structural health monitoring, as well as nanocomposite materials and adhesively bonded joints. Related research projects involve components and structures primarily for the energy sector.